Scientific applications and advantages of a low-energy synchrotron radiation source

U. Arp

National Institute of Standards and Technology, 100 Bureau Dr., Gaithersburg, MD 20899-8410

Abstract. Recent improvements to the synchrotron ultraviolet radiation facility led to unprecedented performance. High injection currents and beam stability, as well as tunable electron energies over a wide range make this storage ring a prime source for synchrotron radiation from the extreme-ultraviolet to far-infrared spectral regions. We will discuss plans to capitalize on this unprecedented performance through implementation of new experimental stations and extension of existing ones. It also will be shown that for applications using extreme-ultraviolet to infrared synchrotron radiation a low electron energy storage ring has distinct advantages.

INTRODUCTION

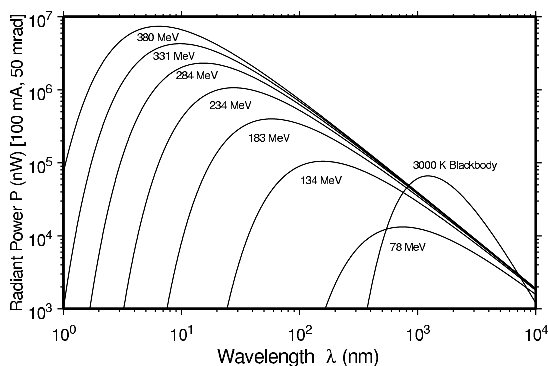

FIGURE 1. Calculated radiant power for SURF at several operating energies compared to a 3000 K blackbody source. Note that above about a 180 MeV the radiant power in the ultraviolet to infrared spectral regions does not depend on the electron energy.

In recent years the number of synchrotron radiation sources has increased considerably worldwide. Most of these new machines are third generation synchrotron radiation sources [1] based on very low emittance storage rings to maximize the available brightness of the emitted photon beam. Several third generation storage rings optimized for the soft or hard x-ray spectral regions are currently in operation. However, a very low emittance storage ring can be realized only for electron energies of 1 GeV or higher.

The very successful application of synchrotron infrared radiation in spectro-microscopy [2, 3, 4, 5] sparked much interest in the long wavelength end of the spectrum. There are, however, difficult technical problems to solve at third generation synchrotron radiation sources in order to use photons in the infrared, visible or ultraviolet spectral regions. The very high brightness results in very high power densities on optical elements that lead to complex and expensive beamline configurations, *e.g.*, at the first infrared beamline built at the Advanced Light Source in Berkeley [6]. Also, an extremely small transverse source size makes the application of novel infrared imaging techniques impossible.

Recent studies using ultraviolet photoelectron emission microscopy (UV-PEEM) have shown promise in imaging of dopant concentration [7, 8, 9, 10, 11] and magnetic structures [12, 13, 14, 15, 16]. UV-PEEM provides very high spatial resolution, because threshold electrons are imaged, which is otherwise only reachable by scanning electron microscopy (SEM). SEM has two disadvantages compared to UV-PEEM: The image acquisition takes several minutes and the high energy electrons cause damage to the sample. PEEM, however, is an imaging technique, which has been used to study dynamic processes, *e.g.* surface catalytic reactions [17, 18] in realtime. In addition, since fairly low energy photons are used, the damage to the sample is limited. UV-PEEM does not in general allow the fine tuning of the excitation energy, but by using tunable ultraviolet synchrotron radiation the contrast in UV-PEEM could be significantly enhanced.

As can be seen in Fig. 1, the radiant power output of a synchrotron radiation source from the ultraviolet to infrared spectral regions does not increase if the electron energy is raised past a threshold level. For the synchrotron ultraviolet radiation facility (SURF) this energy is about 183 MeV. Thus, all the x-ray power a third

CP680, *Application of Accelerators in Research and Industry: 17th Int'l. Conference,* edited by J. L. Duggan and I. L. Morgan
2003 American Institute of Physics 0-7354-0149-7/03/$20.00

generation synchrotron radiation source emits is wasted when doing experiments at longer wavelengths. Getting rid of this higher energy radiation is difficult since a lot of power will be concentrated in a very small area. At a low energy storage ring no significant power will be emitted in the x-ray range, thus eliminating the need for high-power optics.

At SURF many problems can be eliminated through its flexibility: The electron energy is tunable from 10 MeV to about 400 MeV, allowing the fine-tuning of the output spectrum for different applications and the vertical electron beam size can be manipulated from a few 10 μm to several mm. The tunability in energy has advantages for the calibration work done at SURF in the extreme-ultraviolet spectral region, where it helps to reduce higher-order contaminations [19, 20, 21, 22, 23, 24]. Because of the bigger source size at SURF, it is possible to use infrared focal-plane arrays, thus enhancing capabilities for infrared spectro-microscopy.

INFRARED SYNCHROTRON RADIATION IMAGING SPECTRO-MICROSCOPY

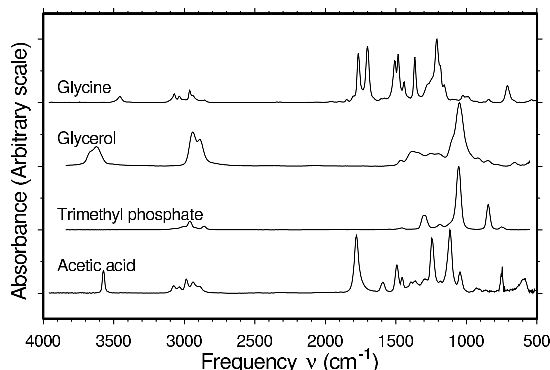

FIGURE 2. Infrared absorption spectra of different molecules taken from the NIST Chemistry WebBook [25].

The main interest in infrared spectro-microscopy is focused on the mid-infrared spectral region, which spawns the wavelength region from about 2.5 μm to 20 μm (wavenumber region 500 cm^{-1} to 4000 cm^{-1}). This is also called the "molecular-fingerprint" region, because of the distinguishably of important molecular groups in this region by their absorption spectra (see Fig. 2 for examples). As can be seen in Fig. 1, the radiant power does not change much in this region with the electron beam energy. Only for very low energies, below 100 MeV, does the spectrum slowly cut-off in the infrared. There is no gain, other than beam stability [26], from operating a storage ring at high energies when utilizing infrared radiation. In fact, the high radiant power in the x-ray spectral region is going to cause trouble in beamline design, thus the optimal infrared synchrotron radiation source operates at low electron energies to minimize heat load and radiation damage problems.

Conventional infrared spectro-microscopy generates spatial information by scanning the sample [2, 3, 4, 5]. This can take more than a day for a large sample. The use of synchrotron radiation instead of a blackbody radiator as a light source reduces these scanning times easily by an order of magnitude. Furthermore, the higher brightness of the synchrotron radiation source enables the collection of images with better spatial resolution. This high brightness results into a small source size, which forbids the application of focal-plane detector arrays for parallel detection.

At SURF the transverse electron beam size can be manipulated in different ways [27]. In standard operation the vertical betatron oscillation is excited [28] and the vertical beam full-width-at-half-maximum (FWHM) is increased to 1 mm. The horizontal beam FWHM is left unchanged by this procedure, except for small coupling effects. In order to increase the brightness and generate a nearly square source the accelerator can be operated with full-coupling instead, resulting in a beam about 1.5 mm wide and 1 mm high [27]. This source is nearly perfect for infrared spectro-microscopy with a focal-plane array and also delivers more photons than a blackbody radiator. At third generation synchrotron radiation sources this is impossible, because of the small transverse electron beam size (*e.g.*, at ELETTRA the source size is 0.140 mm by 0.03 mm [29]).

ULTRAVIOLET SYNCHROTRON RADIATION PHOTOELECTRON EMISSION SPECTROSCOPY

Photoelectron emission microscopy (PEEM) became popular with the introduction of bakable, ultrahigh vacuum compatible instruments suitable for the stringent requirements of surface science [30, 31, 32, 33]. The samples in the microscopes were generally illuminated with ultraviolet (UV) lamps, lacking selectivity in the exciting photon energy. However, using UV light to emit photoelectrons results in very high spatial resolution, below 10 nm [34], because of the low kinetic energy of the threshold photoelectrons, effectively limiting the chromatic focal shift.

Ultraviolet photoelectron emission spectroscopy (UV-PEEM) uses photons for illumination and directly images photoelectrons, thus image acquisition is done in real-time, opening the door for studies of dynamic processes [35]. The "photoelectron-image" is magnified by electron optics and projected onto a screen, which is then

TABLE 1. Imaging techniques for magnetic domains (from [15]). Chem. spec.: Chemical specification; AF-spec.: Antiferromagnetic specification. The remark "Real samples" means that no special preparation is needed.

Method	Excitation	Resolution (nm)	Chem. spec.	AF-spec.	Probing depth (ML)*	Remarks
US-PEEM	SR UV	30 (7)	Some	Yes	—	Real samples
UV-PEEM	UV	30 (7)	No	Yes	—	Real samples
X-PEEM	SR X-ray	100 (20)	Yes	Yes	0.1	Real samples
XSM	SR X-ray	500	Yes	Yes	0.5	Magn. Field
XTM	SR X-ray	20	Yes	Yes	100	Magn. Field Transmission
X-TOPO	SR X-ray	1000	No	Yes	Volume	Magn. Field Transmission
SEMPA	Electrons	50 (10)	No	No	30	

* ML: Monolayer

observed with a charged-coupled device (CCD) camera [36]. The extreme surface sensitivity of UV-PEEM makes it a prime tool for surface science.

The main contrast mechanism is variation of the electron yield [35], which is caused by changes in the electron work function [31]. These changes can be caused by the elemental composition, crystal orientation, and dopant concentration [7, 8, 9, 10, 11]. Contrast can be induced as well by deflection or focusing by topographic relief [37], shadows cast by surface features [35], deflection by surface magnetism [12, 13, 14], and by dichroism in the photoelectron emission [16].

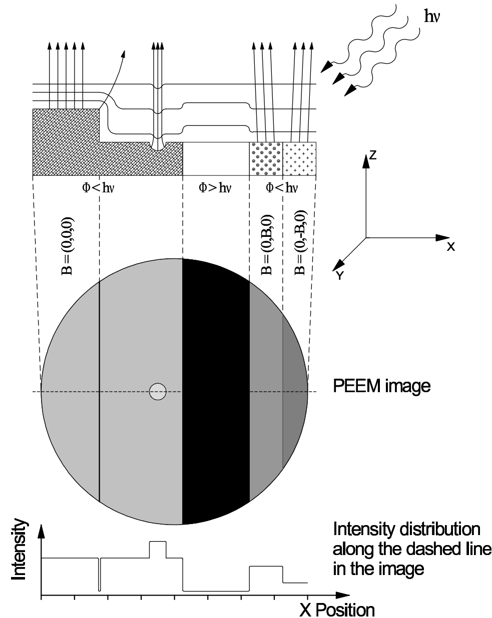

FIGURE 3. Illustration of contrast mechanisms in UV-PEEM. **Top**: Composite surface with electron work function Φ, magnetic field B and illumination $h\nu$. **Middle**: PEEM Image is dark for $\Phi > h\nu$. On the left a step and a depression simulate topographical contrast [35]. On the right non-zero magnetic fields cause Lorentz-contrast by deflecting the photoelectrons. **Bottom**: Expected intensity distribution along the horizontal line cutting through the image.

The topography of the sample is the main contrast mechanism for PEEM with broadband excitation [37]. To extract information on the magnetic state, the topographic signal has to be removed. The different contrast mechanisms are illustrated in Fig. 3.

For similar reasons as in the infrared, a low energy storage ring has advantages in the ultraviolet. Again heat-load problems are absent and there is no need for high-powered optics. Also radiation damage to optical elements will be small. In the UV different window materials with high transmission can be used to eliminate higher orders of the monochromator.

In a recent review article [15] on magnetic imaging several methods were compared: Ultraviolet photoelectron emission microscopy (UV-PEEM), x-ray photoelectron emission microscopy (X-PEEM), x-ray scanning microscopy (XSM), x-ray transmission microscopy (XTM), x-ray topography (X-TOPO), and scanning electron microscopy with polarization analysis (SEMPA). The results of that comparison are summarized in table 1 and in addition the properties for ultraviolet synchrotron radiation photoelectron emission microscopy (US-PEEM) are shown. Using tunable ultraviolet radiation is the preferable technique, as long as no depth information is sought.

EXTREME-ULTRAVIOLET OPTICAL PROPERTIES

For work on extreme-ultraviolet (EUV) optical properties the flexibility of SURF to run at different energies has become essential. It is not possible to completely eliminate higher-order contributions of monochromators, but it is possible to deduce their strength by use of several electron energy and filter material combinations [24]. Only through this flexibility can we fulfill the stringent requirements of EUV lithography in measurement of op-

tical properties. This has become very important in the calibration of photodiodes and measurement of multilayer reflectivities in the EUV spectral range.

ACKNOWLEDGMENTS

Useful discussions on photoelectron emission microscopy with M.E. Kordesch, E.D. Williams, V.W. Ballaroto, and R. Stockbauer, on infrared spectromicroscopy with E.J. Heilweil, J. Dunkers, N. Eidelman, K. Kalasinsky, and C.L. Carr, and on extreme-ultraviolet optical properties with C. Tarrio, S. Grantham, T.B. Lucatorto, and R.E. Vest are gratefully acknowledged.

REFERENCES

1. Schlachter, A. S., and Wuilleumier, F. J., editors, *New directions in research with third-generation soft x-ray synchrotron radiation sources*, vol. 254 of *NATO ASI Series E: Applied Sciences*, Kluwer Academic, Dordrecht, 1994, ISBN 0792326237.
2. Reffner, J. A., Martoglio, P. A., and Williams, G. P., *Rev. Sci. Inst.*, **66**, 1298–1302 (1995).
3. Yarwood, J., Shuttleworth, T., Hasted, J. B., and Nanba, T., *Nature*, **312**, 742–744 (1984).
4. Duncan, W. D., and Williams, G. P., *Appl. Opt.*, **22**, 2914–2923 (1983).
5. Williams, G. P., Takacs, P. Z., Klaffky, R. W., and Shleifer, M., *Nucl. Inst. & Meth. in Phys. Res. A*, **246**, 165–167 (1986).
6. McKinney, W. R., Hirschmugl, C. J., Padmore, H. A., Lauritzen, T., Andresen, N., Andronaco, G., Patton, R., and Fong, M., "First infrared beamline at the ALS: design, construction, and initial commissioning," in *Accelerator-Based Infrared Sources and Applications*, edited by G. P. Williams and P. Dumas, SPIE, Bellingham, WA, 1997, vol. 3153, pp. 57–65.
7. Giesen, M., Phaneuf, R. J., Williams, E. D., and Einstein, T. L., *Surf. Sci.*, **396**, 411–421 (1998).
8. Giesen, M., Phaneuf, R. J., Williams, E. D., Einstein, T. L., and Ibach, H., *Appl. Phys. A*, **64**, 423–430 (1997).
9. Ballarotto, V. W., Siegrist, K., Phaneuf, R. J., Williams, E. D., and Mogren, S., *Surf. Sci.*, **461**, L570–L574 (2000).
10. Ballarotto, V. W., Siegrist, K., Phaneuf, R. J., and Williams, E. D., *J. Appl. Phys.*, **91**, 469–475 (2002).
11. Ballarotto, V. W., Siegrist, K., Phaneuf, R. J., and Williams, E. D., *Appl. Phys. Lett.*, **78**, 3547–3549 (2001).
12. Mundschau, M., Romanowicz, J., Wang, J. Y., Sun, D. L., and Chen, H. C., *J. Vac. Sci. & Tech. B*, **14**, 3126–3130 (1996).
13. Weber, N. B., Bethke, C., and Hillebrecht, F. U., *J. Magn. Magn. Mater.*, **226–230**, 1573–1576 (2001).
14. Schönhense, G., *J. Phys.: Condens. Matter*, **11**, 9517–9547 (1999).
15. Hillebrecht, F. U., *J. Phys.: Condens. Matter*, **13**, 11163–11180 (2001).
16. Marx, G. K. L., Elmers, H. J., and Schönhense, G., *Phys. Rev. Lett.*, **84**, 5888–5891 (2000).
17. Pollmann, M., Bertram, M., and Rotermund, H. H., *Chem. Phys. Lett.*, **346**, 123–128 (2001).
18. Rotermund, H. H., *Phys. Stat. Sol. A*, **188**, 1537–1548 (2001).
19. Tarrio, C., Watts, R. N., Lucatorto, T. B., Haass, M., Callcott, T. A., and Jia, J., *J. X-Ray Sci. & Tech.*, **4**, 96 (1994).
20. Tarrio, C., Watts, R. N., Lucatorto, T. B., Haass, M., Callcott, T. A., and Jia, J., "Improved reflectometry facility at the National Institute of Standards and Technology," in *Multilayer and Grazing Incidence X-Ray/EUV Optics II*, edited by R. B. Hoover and A. B. Walker, SPIE, Bellingham, WA, 1994, vol. 2011, pp. 534–539.
21. Gullikson, E. M., Korde, R., Canfield, L. R., and Vest, R. E., *J. Electron. Spectrosc. Relat. Phenom.*, **80**, 313–316 (1996).
22. Tarrio, C., Lucatorto, T. B., Grantham, S., Squires, M. B., Arp, U., and Deng, L., "Upgrades to the NIST/DARPA EUV reflectometry facility," in *Soft X-Ray and EUV Imaging Systems II*, edited by D. A. Tichenor and J. A. Folta, SPIE, Bellingham, WA, 2001, vol. 4506, pp. 32–38.
23. Tarrio, C., Vest, R. E., and Grantham, S., "Absolute extreme-ultraviolet metrology," in *Harnessing Light: Optical Science and Metrology at NIST*, edited by C. Londono, SPIE, Bellingham, WA, 2001, vol. 4450, pp. 94–107.
24. Grantham, S., Tarrio, C., Squires, M. B., and Lucatorto, T. B., "First results from the updated NIST/DARPA EUV reflectometry facility," in *Emerging Lithographic Technologies VI*, edited by R. L. Engelstad, SPIE, Bellingham, WA, 2002, vol. 4688, pp. 348–353.
25. NIST Chemistry WebBook (2001), URL `http://webbook.nist.gov/chemistry/`.
26. Arp, U., Lucatorto, T. B., Harkay, K., and Kim, K.-J., *Rev. Sci. Inst.*, **73**, 1417–1419 (2002).
27. Arp, U., Friedman, R., Furst, M. L., Makar, S., and Shaw, P.-S., *Metrologia*, **37**, 357–360 (2000).
28. Rakowsky, G., and Hughey, L. R., *IEEE Trans. Nucl. Sci.*, **NS-26**, 3845–3847 (1979).
29. ELLETRA parameters (2002), URL `http://www.elettra.trieste.it/accelerator/parameters.html`.
30. Griffith, O. H., and Rempfer, G. F., *Photoelectron imaging: Photoelectron microscopy and related techniques*, vol. 10 of *Advances in Optical and Electron Microscopy*, Academic Press, New York, 1987.
31. Bethge, H., and Klaua, M., *Ultramicroscopy*, **11**, 207–213 (1983).
32. Telieps, W., and Bauer, E., *Ultramicroscopy*, **17**, 57–65 (1985).
33. Engel, W., Kordesch, M. E., Rotermund, H. H., Kubala, S., and von Oertzen, A., *Ultramicroscopy*, **36**, 148–153 (1991).
34. Rempfer, G. F., and Griffith, O. H., *Ultramicroscopy*, **27**, 273–300 (1989).
35. Kordesch, M. E., *In Situ Real Time Characterization of Thin Films*, John Wiley & Sons, New York, NY, 2001, chap. 8, pp. 217–260.
36. Smith, G. E., *Nucl. Inst. & Meth. in Phys. Res. A*, **471**, 1–5 (2001).
37. Bauer, E., *J. Electron. Spectrosc. Relat. Phenom.*, **114–116**, 975–987 (2001).